P-ISSN 2586-9000
E-ISSN 2586-9027
Homepage : *https://tci-thaijo.org/index.php/SciTechAsia* **Science & Technology Asia**
Vol.22 No.4 October - December 2017 Page: [71 – 85]

Original research article

Free Convection Flow over a Vertical Flat Plate in Nanofluid Porous Media Containing Gyrotactic Microorganisms with Prescribed Density Motile Microorganisms Flux

A. Mahdy[1,*]
[1]*Mathematics Department, Faculty of Science, South Valley University, Qena 83523, Egypt*

Received 21 February 2017; Received in revised form 20 March 2017
Accepted 31 March 2017; Available online 30 June 2017

ABSTRACT

Our present investigation aimed to examine the natural convection boundary layer flow of nanofluids over a vertical flat plate embedded in a saturated Darcy porous medium containing gyrotactic microorganisms. For carrying out the numerical solution, two steps are performed. The governing partial differential equations are firstly simplified into a set of highly coupled nonlinear ordinary differential equations by suitable similarity variables, and then numerically solved by applying the cubic spline collocation technique. The obtained similarity solution depends on non-dimensional parameters, i.e., the bioconvection Lewis number, bioconvection Rayleigh number, bioconvection Peclet number, Brownian motion parameter, the Buoyancy ratio, the thermophoresis parameter, the power-law variation index, and the Lewis number. A comprehensive numerical computation is carried out for various values of the parameters that describe the flow characteristics. Rescaled velocity and temperature distributions are found to be depending strongly on the bioconvection Rayleigh number and power-law variation index parameter. For making the result more reliable a comparison has been shown in the present work with existing results for some special values of governing parameters and the results are found to be in excellent accuracy.

Keywords: Surface heat flux; Bioconvection; Gyrotactic microorganisms; Porous media; Nanofluid; Boundary layer.

***Corresponding author:** mahdy@svu.edu.eg **doi:** 10.14456/tijsat.2017.20

1. Introduction

Natural convection flow is often encountered in cooling of nuclear reactors or in the study of the structure of stars and planets. In many practical fields, we found significant temperature differences between the surface of the hot body and the free stream. These temperature differences cause density gradients in the fluid medium and in the presence of gravitational force free convection affects become important. Along with the natural convection flow the phenomenon of mass transfer is also very common in the theories of stellar structure. In many applications of practical importance, the surface temperature is non-uniform. The case of uniform surface heat flux has great importance in engineering applications. Some researchers have studied natural convection flow for a surface which exhibits the uniform surface heat flux [1-7]. Heat transfer is an important process in Physics and Engineering, since the conventional heat transfer in fluids such as water, mineral oil and ethylene glycol are poor conductors of heat compared to those of most solids. Convective heat transfer can be enhanced passively by changing flow geometry, boundary conditions, or by enhancing thermal conductivity of the fluid. Consequently improvements in heat transfer characteristics will improve the efficiency of many processes. A nanofluid is a new class of heat transfer fluids that contains a base fluid and solid nanoparticles of diameter 1–100 nm [8-16]. The use of additives is a technique applied to enhance the heat transfer performance of base fluids. Nanofluids have been shown to increase the thermal conductivity and convective heat transfer performance of the base liquid. Thus nanofluids have many applications in industry such as coolants, lubricants, heat exchangers, micro channel heat sinks and many others. A comprehensive survey of convective transport was presented by Buongiorno [17] by pointing out various facts concerning nanofluids. The author discussed seven possible mechanisms associating convection of nanofluids through movement of nanoparticles in the base fluid. Among the investigated mechanisms, the thermophoresis and the Brownian diffusion were found important. Moreover, he reported that the nanoparticles within the base fluid are subject to forces including thermophoresis and Brownian motion forces. The thermophoresis acts against temperature gradient, meaning that the particles tend to move from hot regions to cold ones. In addition, the Brownian motion tends to move the particles from high concentration areas to low concentration areas. Since microorganisms have to be able to live in the base fluid, the base fluid has to be water. The phenomenon of bioconvection in nanofluid convection which is the focus of the present work is driven by the presence of denser microorganisms accumulating on the surface of lighter water. As the heavier microorganisms sink into the water, they are replenished by upward swimming micro-organisms, thus establishing a bio-convection process within the system. The process is a mesoscale phenomenon in which the motion of motile microorganisms induces a macroscopic motion (convection). Unlike the motile microorganisms, the nanoparticles are not self-propelled, and their motion is driven by Brownian motion and thermophoresis occurring in the nanofluid. Thus the motion of the motile microorganisms is independent of the motion of nanoparticles. Bioconvection has many applications in biological systems and Biotechnology. The term bioconvection refers to a macroscopic convection motion of fluid caused by the density gradient created by collective swimming of motile microorganisms [18-23]. Adding microorganisms to a nanofluid increases its stability as a suspension [24],

and could avoid nanoparticles from agglomerating and aggregating. A detailed discussion [25-35] of bioconvection in suspensions of oxytactic bacteria is made for the onset of bioconvection in a suspension of gyrotactic/oxytactic microorganisms in different cases. They performed stability analysis and determined the effect of small solid particles in a dilute suspension containing gyrotactic microorganisms, and introduced the concept of effective diffusivity to determine the effect of bioconvection on small solid particles.

Considering the contributions mentioned above, our objective in the present paper is to analyze the steady natural convection flow of a nanofluid over a vertical plate embedded in a nanofluid saturated porous medium that contains gyrotactic microorganisms subjected to the surface heat, nanoparticle volume fraction and motile microorganisms fluxes. The nanofluid model, utilized in the present study, incorporates the dynamic effects of nanoparticles, including the Brownian motion and thermophoresis.

2. Flow analysis

A two-dimensional natural convection boundary layer flows along a vertical plate placed in a porous medium saturated with a nanofluid containing gyrotactic microorganisms. It is assumed that the flow is incompressible and steady- state. The plate surface is imposed to the surface heat, the nanoparticle and density of microorganisms fluxes. The coordinate system is chosen such that the x - axis is aligned with the flow on the plate. The ambient values of the temperature, nanoparticle concentration and density of microorganisms are denoted by T_∞ , C_∞ and N_∞ , respectively, as y tends to infinity. The flow in the homogeneous porous medium with the porosity ò and the permeability K is considered as Darcy flow, and the Oberbeck-Boussinesq approximation is employed. In addition, the nanoparticle suspension is assumed to be stable (there is no nanoparticle agglomeration). The presence of nanoparticles is assumed to have no effect on the direction in which microorganisms swim and on their swimming velocity. This is a reasonable assumption if the nanoparticle suspension is dilute (nanoparticle concentration is lower than 1%). Bioconvection induced flow only takes place in a dilute suspension of nanoparticles; otherwise, a large concentration of nanoparticles would result in a large suspension viscosity, which would suppress bioconvection. With the standard boundary layer approximations, the steady-state conservation of the total mass, the momentum, the energy, conservation of gyrotactic microorganisms and the conservation of nanoparticles for nanofluids over a heated surface embedded in a saturated porous medium are presented in non-dimensional form as [2.7, 2.10].

$$\frac{\partial u}{\partial x} + \frac{\partial v}{\partial y} = 0 \tag{2.1}$$

$$\frac{\partial P}{\partial y} = 0 \tag{2.2}$$

$$\frac{m}{K}u = -\frac{\partial P}{\partial x} + (1 - C_\infty)g\beta_{f\infty}(T - T_\infty) - (\rho_p - \rho_{f\infty})g(C - C_\infty)$$

$$-(\rho_{m\infty} - \rho_\infty)gg(N - N_\infty) \tag{2.3}$$

$$u\frac{\partial T}{\partial x}+v\frac{\partial T}{\partial y}=\alpha\frac{\partial^2 T}{\partial y^2}+\tau\left\{D\frac{\partial C}{\partial y}\frac{\partial T}{\partial y}+\frac{D_T}{T_\infty}\left(\frac{\partial T}{\partial y}\right)^2\right\} \quad (2.4)$$

$$u\frac{\partial C}{\partial x}+v\frac{\partial C}{\partial y}=\varepsilon\left\{D\frac{\partial^2 C}{\partial y^2}+\frac{D_T}{T_\infty}\frac{\partial^2 T}{\partial y^2}\right\} \quad (2.5)$$

$$u\frac{\partial N}{\partial x}+v\frac{\partial N}{\partial y}+\frac{bW}{\Delta C}\frac{\partial}{\partial y}\left\{N\frac{\partial C}{\partial y}\right\}=D_m\frac{\partial^2 N}{\partial y^2} \quad (2.6)$$

In previous equations 2.1 – 2.6 u and v are the velocity components along the x and y axis, μ is the dynamic viscosity of the fluid, β is the volumetric expansion coefficient, ρ_f is the density of the base fluid, ρ_p is the density of nanoparticles, $\rho_{m\infty}$ is the microorganism density, g is the average volume of microorganisms; W the constant maximum cell swimming speed, K is the Darcy permeability of the porous medium; ε is the porosity; D, D_T, D_n are the Brownian, Thermophoretic diffusion and diffusivity of microorganisms coefficients

$\tau = \varepsilon(\rho c)_p / (\rho c)_f$ is the ratio of effective heat capacity of the nanoparticle material to the heat capacity of the fluid, and $\alpha = k/(\rho c)_f$ is the effective thermal diffusivity. Based on the problem description, the dimensional boundary conditions are shown as Eq. 7a and 7b.

$$v=0,\quad \frac{\partial T}{\partial y}=-\frac{q_w}{k},\quad \frac{\partial C}{\partial y}=-\frac{q_m}{D},\quad \frac{\partial N}{\partial y}=-\frac{q_n}{D_n},\quad y=0,\quad x\neq 0 \quad (2.7a)$$

$$u\to 0,\quad T\to T_\infty,\quad C\to C_\infty,\quad N\to N_\infty,\quad y\to\infty \quad (2.8b)$$

where q_w is the surface heat flux, q_m is the surface nanoparticle flux and q_n is the density of microorganisms flux. The fluxes are assumed to be proportional to x^l, i.e., $q_w = ax^l$, $q_m = bx^l$ and $q_n = cx^l$, where the exponent l is a real value.

The pressure P can be eliminated from Eq. 2.2 and 2.3 by cross-differentiation, and the continuity equation will be automatically satisfied by introducing the following stream function

$$u=\frac{\partial\psi}{\partial y},\quad v=-\frac{\partial\psi}{\partial x}$$

Now, the governing differential equations can be reduced to the differential equations 2.8 – 2.11.

$$\frac{\partial^2\psi}{\partial y^2}=\frac{(1-C_\infty)Kg\beta\rho_{f\infty}}{\mu}\frac{\partial T}{\partial y}-\frac{(\rho_p-\rho_{f\infty})Kg}{\mu}\frac{\partial C}{\partial y}-\frac{(\rho_{m\infty}-\rho_\infty)Kgg}{\mu}\frac{\partial N}{\partial y} \quad (2.8)$$

$$\frac{\partial\psi}{\partial y}\frac{\partial T}{\partial x}-\frac{\partial\psi}{\partial x}\frac{\partial T}{\partial y}=\alpha\frac{\partial^2 T}{\partial y^2}+\tau\left\{D\frac{\partial C}{\partial y}\frac{\partial T}{\partial y}+\frac{D_T}{T_\infty}\left(\frac{\partial T}{\partial y}\right)^2\right\} \quad (2.9)$$

$$\frac{\partial\psi}{\partial y}\frac{\partial C}{\partial x}-\frac{\partial\psi}{\partial x}\frac{\partial C}{\partial y}=\varepsilon\left\{D\frac{\partial^2 C}{\partial y^2}+\frac{D_T}{T_\infty}\frac{\partial^2 T}{\partial y^2}\right\} \quad (2.10)$$

$$\frac{\partial\psi}{\partial y}\frac{\partial N}{\partial x}-\frac{\partial\psi}{\partial x}\frac{\partial N}{\partial y}+\frac{bW}{\Delta C}\frac{\partial}{\partial y}\left\{N\frac{\partial C}{\partial y}\right\}=D_m\frac{\partial^2 N}{\partial y^2} \quad (2.11)$$

To simplify the system of Equations

(2.8) – (2.11) and attain a similarity solution to these equations subjected to boundary condition equation (2.7), the similarity variables are given by

$$h = \frac{y}{x} Ra_x^{1/3}, \qquad y = aRa_x^{1/3} F(h), \qquad q(h) = \frac{k(T - T_\infty)}{q_w x} Ra_x^{1/3}$$

$$f = \frac{D(C - C_\infty)}{q_m x} Ra_x^{1/3}, \qquad c = \frac{D^{\hat{a}}(N - N_\infty)}{q_n x} Ra_x^{1/3}, \qquad Ra_x = \frac{(1 - C_\infty) r_{f\infty} g b q_w}{m a k} x \tag{2.12}$$

The governing equations can be reduced to four coupled ordinary differential equations. Applying equation 2.12 on equations 2.8 – 2.11 and boundary condition equation 2.7 yields the following ordinary differential equations

$$F''' - q' + N_r f' + R_b c' = 0 \tag{2.13}$$

$$q'' + \frac{l+2}{3} F q' - \frac{2l+1}{3} F' q + N_b f' q' + N_t q'^2 = 0 \tag{2.14}$$

$$f'' + \frac{l+2}{3} L_e F f' - \frac{2l+1}{3} L_e F' f + \frac{N_t}{N_b} q'' = 0 \tag{2.15}$$

$$c'' + \frac{l+2}{3} L_b F c' - \frac{2l+1}{3} L_b F' c - Pe\left(c' f' + f'(c + A)\right) = 0 \tag{2.16}$$

Subject to the dimensionless boundary conditions

$$\begin{aligned} &F(h) = 0, && q'(h) = -1, && f'(h) = -1, && c'(h) = -1, && h = 0 \\ &F'(h) \to 0, && q(h) \to 0, && f(h) \to 0, && c(h) \to 0, && h \to \infty \end{aligned} \tag{2.17}$$

The primes denote differentiation with respect to h . In addition, in Eqs. (2.8)–(2.12), Ra is the thermal Rayleigh number, R_b is the bioconvection Rayleigh number, N_r is the buoyancy ratio parameter, N_t is a modified diffusivity ratio parameter (somewhat similar to the Soret parameter that arises in cross-diffusion phenomena in solutions), N_b is the Brownian motion parameter, the parameter L_e is the traditional Lewis number (the ratio of the Schmidt number to the Prandtl number Pr), L_b is the bioconvection Lewis number, P_e is the bioconvection Péclet number, and A is the bioconvection constant, Furthermore, these dimensionless parameters are defined as

$$R_b = \frac{(r_{m\infty} - r_f) g k q_n}{(1 - C_\infty) r_{f\infty} b D^{\hat{a}} q_w}, \qquad N_r = \frac{(r_p - r_{f\infty}) k q_m}{(1 - C_\infty) D r_{f\infty} b q_w}$$

$$N_t = \frac{\grave{o}(rc)_p \bar{D} q_w x}{(rc)_f a k T_\infty Ra_x^{1/3}}, \qquad N_b = \frac{\grave{o}(rc)_p q_m x}{(rc)_f a Ra_x^{1/3}}, \qquad L_e = \frac{a}{\grave{o} D}$$

$$L_b = \frac{a}{D^{\hat{a}}}, \qquad P_e = \frac{b W q_m x}{D^{\hat{a}} D D C Ra_x^{1/3}}, \qquad A = \frac{D^{\hat{a}} N_\infty Ra_x^{1/3}}{q_n x}$$

The results of practical interest in many applications are the local Nusselt Number Nu_x, the local Sherwood number Sh_x and the local density number of the motile microorganisms Nn_x which are defined as equation 2.18.

$$Nu_x = \frac{xq_w}{k(T_w - T_\infty)}, \qquad Sh_x = \frac{xq_m}{D(C_w - C_\infty)} \qquad Nn_x = \frac{xq_n}{D^{\hat{}}(N_w - N_\infty)} \tag{2.18}$$

where q_w, q_m and q_n are the wall heat, the wall mass and the wall motile microorganisms fluxes, respectively, with the similarity transforms introduced in Eq. (2.12), the local Nusselt number (Nu_x), local Sherwood number (Sh_x) and the local density of the motile microorganisms number (Nn_r) are obtained as follows:

$$Nu_x = Ra^{1/3}\frac{1}{q(0)}, \qquad Sh_x = Ra^{1/3}\frac{1}{f(0)}, \qquad Nn_x = Ra^{1/3}\frac{1}{c(0)} \tag{2.19}$$

Furthermore, the reduced local Nusselt number (Nu_r), Sherwood number (Sh_r) and reduced density of the motile microorganisms number (Nn_r) can be written as:

$$Nu_r = \frac{Nu_x}{Ra_x^{1/3}} = \frac{1}{q(0)}, \qquad Sh_r = \frac{Sh_x}{Ra_x^{1/3}} = \frac{1}{f(0)}, \qquad Nn_r = \frac{Nn_x}{Ra_x^{1/3}} = \frac{1}{c(0)} \tag{2.20}$$

3. Numerical method

The obtained transformed governing differential equations, equations (2.13) - (2.16), subjected to the associated boundary conditions, Eq. (2.17), are solved by applying the cubic spline collocation technique [36-38]. The velocity F ¢ is calculated from the momentum equation, Eq. (13). Moreover, the Simpson's rule for variable grids is used to calculate the value of F at every position from the boundary conditions, Eq. (2.17). At every position, the iteration process continues until the convergence criterion for all the variables, 10^{-6}, is achieved (a maximum relative error of 10^{-6} is used as the stopping criteria for the iterations). Variable grids with 400 grid points are used in the h -direction. The optimum value of boundary layer thickness is used. To assess the accuracy of the solution, the present results are compared with the results obtained by other researchers. Table 1 shows the numerical values of reduced Nusselt number $\frac{1}{q(0)}$ for different values of l with $N_t = Rb = 0$ and $N_r = N_b = 0$, the conditions for natural convection heat of a vertical plate of Newtonian fluids in porous media with surface heat flux. It is shown that the present results are in excellent agreement with the results reported by Cheng [1], Hsieh et al. [38] and Noghrehabadi et al. [7]. Table 2 displays the numerical values of reduced Nusselt number $\frac{1}{q(0)}$ for different values of N_t, N_b, N_r and L_e.

Table 1. Comparison results for reduced Nusselt number.

l	Hsieh et al. [38]	Noghrehabadi et al. [7]	Cheng [1]	Present
-0.5	0.5818		0.5818	0.581780
0	0.771 5	0.771 545	0.771 5	0.771 50
0.5	0.8998		0.8998	0.899811
1	1.0000		1.0000	1.000000

Table 2. Comparison results for reduced Nusselt number for different values of N_t, N_b, N_r and Le.

N_b	N_t	$N_r = 0.1$				$N_r = 0.3$			
		$Le = 10$		$Le = 50$		$Le = 10$		$Le = 50$	
		Ref. [7]	**present**	**Ref. [7]**	**present**	**Ref. [7]**	**present**	**Ref. [7]**	**present**
0.1	0.1	0.535 23	0.535 226	0.545 14	0.545 133	0.528 09	0.5280841	0.543 64	0.543 631
	0.2	0.504 76	0.504 759	0.515 36	0.515 358	0.495 68	0.495681	0.513 45	0.513 450
	0.3	0.474 74	0.474 742	0.485 19	0.485 187	0.464 51	0.464 503	0.483 04	0.483 034
	0.4	0.445 05	0.445 046	0.454 54	0.454 544	0.434 33	0.434 326	0.452 30	0.452 294
	0.5	0.415 55	0.415 548	0.423 36	0.423 361	0.404 93	0.404 925	0.421 15	0.421 149
0.3	0.1	0.512 56	0.512 553	0.532 794	0.532 80	0.507 92	0.507 913	0.531 73	0.531 730
	0.2	0.484 06	0.484 062	0.503 650	0.503 65	0.479 16	0.479 161	0.502 52	0.502 521
	0.3	0.455 68	0.455 680	0.474 038	0.474 04	0.450 73	0.450 733	0.472 90	0.472 895
	0.4	0.427 32	0.427 315	0.443 890	0.443 89	0.422 51	0.422 505	0.442 78	0.442 777
	0.5	0.398 88	0.398 819	0.413 147	0.413 15	0.394 36	0.394 364	0.412 10	0.412 104
0.5	0.1	0.490 87	0.490 864	0.520 814	0.520 86	0.486 88	0.486 878	0.519 83	0.519 827
	0.2	0.463 56	0.463 559	0.492 140	0.492 14	0.459 62	0.459 621	0.491 16	0.491 160
	0.3	0.436 25	0.436 249	0.462 974	0.462 97	0.432 46	0.432 464	0.462 03	0.462 027
	0.4	0.408 85	0.408 855	0.433 249	0.433 25	0.405 31	0.405 309	0.432 36	0.432 359
	0.5	0.381 30	0.381 304	0.402912	0.40291	0.378 07	0.378 071	0.402 10	0.402 100

4. Results and discussion

For illustrations of the results, numerical values are plotted in Figs. 2–11 and Tables 1-4 and a detailed discussion on the effects of the governing parameters on the rescaled velocity, temperature, nanoparticle volume fraction and rescaled density of motile microorganisms distributions is presented. Since the thermal diffusivity of most nanofluids is much higher than the Brownian diffusion coefficient, the values of the Lewis number are comparatively high ($Le > 1$), the values of $Le = 10$ and $Le = 50$ are examined in the present study. The choice of values for N_r, N_b and N_t is based on those values utilized by Nield and Kuznetsov for the case with the isothermal wall boundary condition. With the same values of N_r, N_b and N_t the present work with the heat flux boundary condition is viewed in proper perspective with the results for an isothermal plate. The values of the reduced density of the motile microorganisms number $\frac{1}{c(0)}$ is shown in Tables 3 and 4, respectively, for selected combinations of l, N_t, N_b, R_b, N_r, Pe and Lb when $Le = 10$. The results in Tables 3 and 4 indicate that the increase in the Brownian motion parameter, the thermophoresis parameter, bioconvection Peclet number, power-law variation index l, or the

Bioconvection Lewis number increases the reduced density of the motile micro-organisms number. The influence of the bioconvection Rayleigh number and buoyancy ratio parameter tend to decrease the reduced density of the motile microorganisms number. The variations of the reduced density of the motile microorganisms number in Tables 3 and 4 reveals that the effects of the Brownian motion and the thermophoresis parameters on the reduced density of the motile microorganisms number are more than that of the buoyancy ratio parameter. The reference case for these figures is $Le = 10$, $A = 0.2$, $Pe = 0.7$, $Nt = 0.4$, $Lb = 5$, $Nr = 0.2$, $Nb = 0.9$ and $Rb = 0.5$ with $l = -0.5$ and $l = 0.5$.

Table 3. Effects of Nt, Nb, Rb and Lb on reduced density of the motile microorganisms number.

Nt	Nb	$Rb = 0.0$		$Rb = 0.2$		$Rb = 0.4$	
		$Lb = 1.0$	$Lb = 5.0$	$Lb = 1.0$	$Lb = 5.0$	$Lb = 1.0$	$Lb = 5.0$
0.1	0.6	1.498210	2.973360	1.466154	2.934053	1.433158	2.893384
	0.8	1.514177	3.011055	1.483436	2.973394	1.451930	2.934546
	1.0	1.529695	3.047804	1.500177	3.011662	1.470028	2.974490
	1.2	1.544892	3.083813	1.516507	3.049093	1.487606	3.013469
0.4	0.6	1.557590	3.098383	1.530432	3.064045	1.502860	3.028800
	0.8	1.575102	3.138197	1.549044	3.105242	1.522676	3.071497
	1.0	1.591765	3.176423	1.566744	3.144763	1.541492	3.112412
	1.2	1.607916	3.213619	1.583864	3.183168	1.559650	3.152102
1.0	0.6	1.692886	3.372156	1.673799	3.346362	1.654829	3.320208
	0.8	1.710931	3.411584	1.692513	3.386583	1.674229	3.361270
	1.0	1.728246	3.449762	1.710507	3.425617	1.692905	3.401147
	1.2	1.745109	3.487110	1.728013	3.463755	1.711075	3.440137

Table 4. Effects of Nr, l and Pe on reduced density of the motile microorganisms number.

Nr	$Pe = 0.1$			$Pe = 0.9$		
	$l = -0.5$	$l = 0$	$l = 0.5$	$l = -0.5$	$l = 0$	$l = 0.5$
0.00	2.009112	2.348769	2.629976	2.960281	3.327859	3.639561
0.05	2.006487	2.343615	2.623247	2.957139	3.321847	3.6317842
0.10	2.003861	2.338437	2.616482	2.953991	3.315807	3.6239638
0.15	2.001227	2.333239	2.609679	2.950835	3.309737	3.6161039
0.20	1.998588	2.328018	2.602843	2.947672	3.302712	3.6081945
0.25	1.995944	2.322762	2.595964	2.944501	3.299217	3.6002381

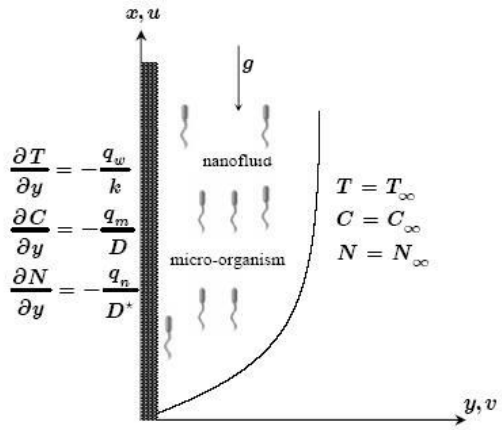

Fig. 1. Schematic diagram of the problem.

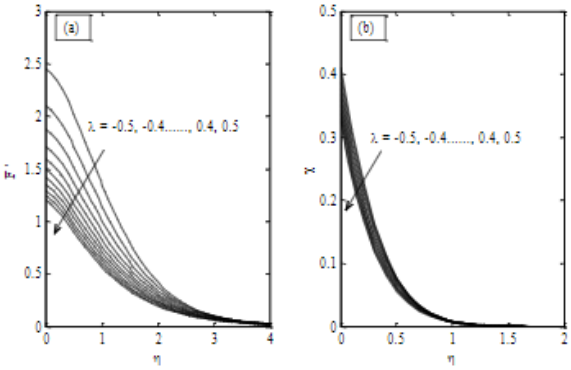

Fig. 2. Effect of power-law variation on (a) Velocity (b) Density of motile microorganisms distributions.

The effect of power-law variation parameter l on dimensionless velocity, temperature, nanoparticle volume fraction and density of motile microorganisms distributions is illustrated in Figs. 2 (a, b), and 3(a, b). As it is observed as l increases all of dimensionless velocity, temperature, nanoparticle volume fraction and density of motile microorganisms distributions decrease. The Brownian motion parameter can be described as the ratio of the nanoparticle diffusion, which is due to the Brownian motion effect, to the thermal diffusion in the nanofluid. Therefore, it is expected that the Brownian motion parameter increases with an increase in the difference between the nanoparticle volume fractions at the wall and ambient. Based on the Einstein-Stokes equation, the Brownian motion is proportional to the inverse of the particle diameter [17]. Hence, as the particle diameter decreases, the Brownian motion increases. The profiles of the temperature and the nanoparticle volume fractions, for different values of the Brownian motion parameter are depicted in Fig. 4(a, b), when $l = -0.5$ and $l = 0.5$. This figure reveals that the increase in N_b increases the dimensionless temperature profiles whereas it decreases the nanoparticle concentration profiles. Comparisons between Fig. 3 (a, b) shows that the effects of variations of N_b on the variations of concentration profiles are much higher than those effects on the temperature profiles. Generally, the increase in N_b tends to decrease the nanoparticle concentration, as shown in Fig. 4(b). The diffusion of nanoparticles into the fluid increases with the increase in N_b , and thereby, the temperature profiles are increased, as shown in Fig. 4(a). It is worth mentioning that the consideration of additional heat transfer mechanisms in the convective heat transfer problems has been further developed by Buongiorno [17] who discussed seven possible mechanisms which affect the convection of nanofluids because of the movement of nanoparticles in the base fluid. Of all the mechanisms, the thermophoresis and the Brownian diffusion are found to be important. The thermophoresis parameter N_t can be described as the ratio of the nanoparticle diffusion, which is due to the thermophoresis effect, to the thermal diffusion in the nanofluid. According to Buongiorno's report, the solid particles in the fluid experience a force in the direction opposite to the imposed temperature gradient. Therefore, the particles tend to

move from hot to cold. The increase in the nanoparticle concentration by the increase in the thermophoresis effect results in the increase in the temperature profiles and consequently the increase in the velocity profiles. The thermophoresis parameter is independent of the particle diameter in the case of very small particles. The profiles of the temperature and the nanoparticle volume fraction, for different values of N_t are plotted in Fig. 5(a, b) when l = - **0.5** and l = **0.5** . This figure reveals that the increase in N_t increases the magnitude of the dimensionless temperature Fig. 5(a), and the magnitude of the concentration profiles. This is because the thermophoresis force, which tends to move particles from the hot zone to the cold zone, increases with the increase in N_t, which results in that the increase in the thermophoresis force increases the nanoparticle concentration, as seen in Fig. 5(b). Furthermore, the increase in the nanoparticle diffusion into the fluid increases the magnitude of the dimensionless temperature, as shown in Fig. 4(a). In addition, increasing the power-law variation parameter l tends to increase the dimensionless temperature and the concentration profiles.

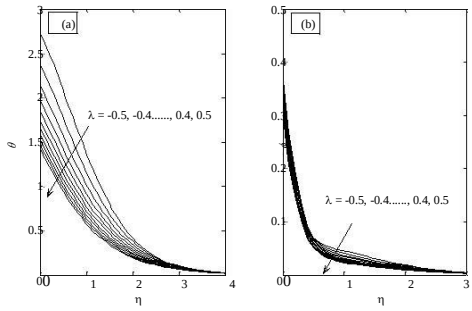

Fig. 3. Effect of power-law variation on (a) Temperature (b) Nanoparticle volume fraction distributions.

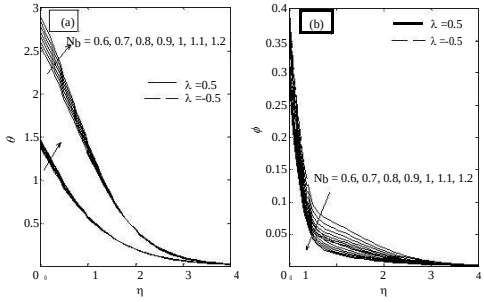

Fig. 4. Effect of Brownian motion parameter on (a) Temperature (b) Nanoparticle volume fraction distributions.

Figs. 6 and 7 illustrate the variation of the dimensionless velocity, the motile micro-organisms, the dimensionless temperature and the nanoparticle volume fractions for different values of buoyancy ratio N_r when l = - **0.5** and l = **0.5** . The dimensionless velocity at the surface is found to be higher. It can be observed that the dimensionless velocity distribution decreases with an increase in the buoyancy ratio. Furthermore, density of motile microorganisms, temperature and nanoparticle volume fractions profiles increase with increasing buoyancy ratio parameter. The bio-convection Rayleigh number has the same effect as the buoyancy ratio parameter on dimensionless velocity, i.e. increasing the bioconvection Rayleigh number tends to decrease the dimensionless velocity profile, whereas the density of motile micro-organisms distribution increases with the increase in bioconvection Rayleigh number as observed in Fig. 8(a, b). Fig. 9 displays the effect of the Lewis number Le on the concentration profiles 9(a) and effect of the bioconvection Peclet number on density of motile microorganisms profile 9(b). The Lewis number is an important parameter in heat and mass transfer processes as it characterizes the ratio of thicknesses of the thermal and concentration boundary layers. Its effect on the species concentration has similarities to the Prandtl number effect on the temperature.

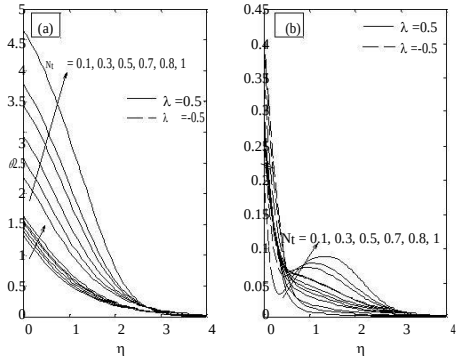

Fig. 5. Effect of thermophoresis parameter on (a) Temperature (b) Nanoparticle volume fraction distributions.

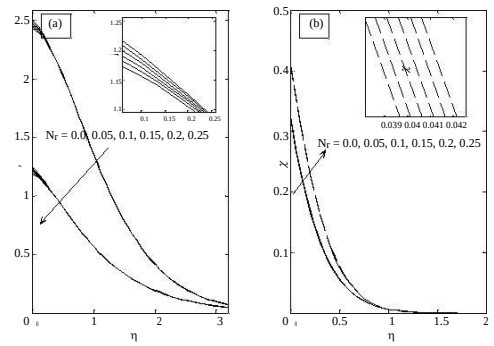

Fig. 6. Effect of buoyancy ratio parameter on (a) Velocity (b) Density of motile microorganisms distributions.

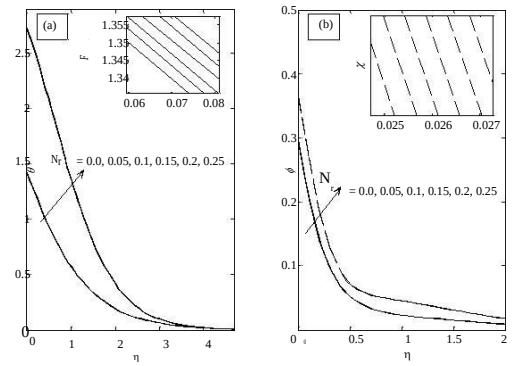

Fig. 7. Effect of buoyancy ratio parameter on (a) Temperature (b) Nanoparticle volume fraction distributions.

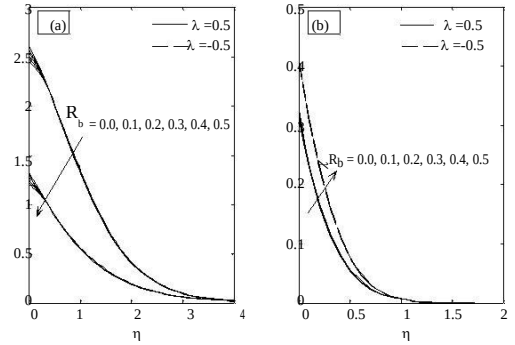

Fig. 8. Effect of bioconvection Rayleigh number on (a) Velocity (b) Density of motile microorganisms distributions.

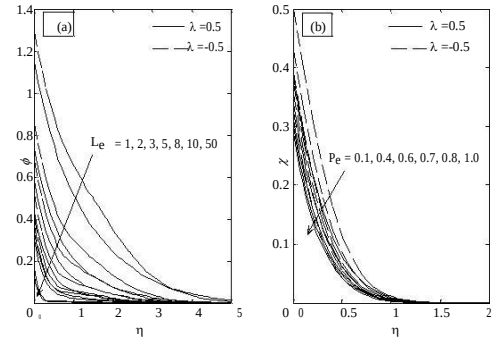

Fig. 9. (a) Effect of Lewis number on nanoparticle volume fraction on (b) Effect of bioconvection Peclet number on density of motile microorganisms distributions.

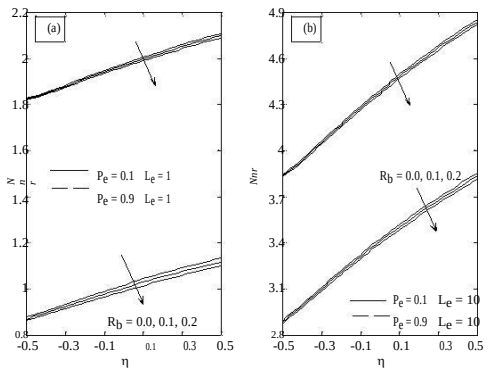

Fig. 10. Variation of density of motile microorganisms numbers against ***l*** for different

R b , Pe (a) ***Lb* = 1** (b) ***Lb* = 10.**

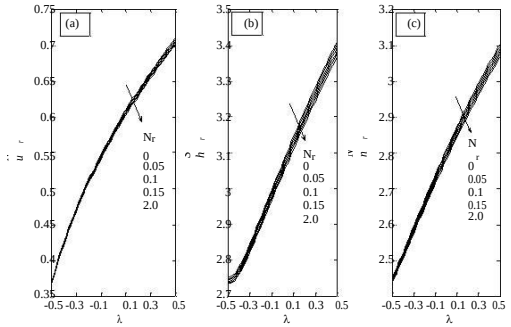

Fig. 11. Variation of reduced (a) Nusselt (b) Sherwood (c) Density of motile microorganisms numbers against l for different N_r.

Therefore, as expected, it is observed that as the Lewis number increases, the concentration decreases. In addition, increasing the Lewis number tends to decrease the concentration boundary layer thickness, thus increasing the mass transfer rate between the porous medium and the surface. The effect of the bioconvection Peclet number is similar to the effect of the Lewis number on concentration, i.e. as the bioconvection Peclet number increases, the concentration thickness for the dimension-less density of motile micrrorganisms profile decreases. Fig. 10 (a, b) depicts the variation of reduced density of motile micrrorganisms against power-law variation l for different values of bioconvection Rayleigh number when

$P_e = 0.1, P_e = 0.9, L_e = 1,$ and $L_e = 10$.

As can be seen, the reduced density of the motile micrrorganisms number increases with increasing bioconvection Peclet numbers, Lewis numbers, and power-law variation parameters, but it decreases with increasing bioconvection Rayleigh numbers. From Fig. 11 (a, b, c) we see that the reduced Nusselt number, reduced Sherwood number and reduced density of motile micrrorganisms number decrease with an increasing buoyancy ratio parameter.

5. Conclusions

The boundary layer natural convection flow of a water-based nanofluid containing motile microorganisms past a vertical permeable flat plate with surface heat, mass, motile microorganisms fluxes is investigated numerically. The model used for the nanofluid incorporates the effects of Brownian motion and thermophoresis. Pertinent results are presented graphically and tabulated and discussed quantitatively with respect to variation in the controlling parameters. The following important results are drawn from our contribution:

1. The rescaled density of motile microorganisms profile decreases with bioconvection Lewis numbers, power-law variation parameter and bioconvection Peclet number.
2. The reduced density of motile microorganisms number decreases with an increase in buoyancy ratio parameter and bioconvection Rayleigh number, whereas it increases with increasing bioconvection Peclet number, bioconvection Lewis number and power-law variation parameter.
3. The reduced Nusselt number decreases with an increase in Brownian motion, thermophoresis and buoyancy ratio parameters.
4. Both of reduced density of motile microorganisms number increases with an increase in Brownian motion and thermophoresis.
5. Rescaled velocity and temperature profiles depend strongly on the bioconvection Rayleigh number and power-law variation index parameter.

Nomenclature

a, b, c constants

A microorganisms concentration difference parameter

C nanoparticle volume fraction D Brownian diffusion coefficient

$\bar{D}$ thermophoretic diffusion coefficient

$D_{å}$ diffusivity of microorganisms

F dimensionless stream function

g Acceleration due to gravity

k thermal conductivity

K permeability of porous medium

L_b bioconvection Lewis number

L_e Lewis number

N concentration of microorganisms

N_b Brownian motion parameter

N_r buoyancy ratio

N_t thermophoresis parameter

$N n_x$ the density number of motile microorganisms

$N u_x$ Nusselt number

P pressure

P_e bioconvection Peclet number

q_m surface mass flux

q_n surface motile microorganisms flux

q_w surface heat flux

$R a$ Rayleigh number

R_b bioconvection Rayleigh number

Sh_x Sherwood number

T temperature

W constant maximum cell swimming speed

(u, v) velocity components of the fluid

(x, y) coordinate axis

Greek symbols

a Thermal diffusivity of porous media f dimensionless nanoparticle volume fraction

b volumetric expansion coefficient

q dimensionless temperature

h similarity variable

c dimensionless density of motile microorganisms

$(rc)_p$ effective heat capacity of nanoparticle material

$(rc)_f$ heat capacity of the fluid

r_f density of the fluid

r_p nanoparticle mass density

t the ratio between the effective heat capacity of the nanoparticle material and heat capacity of the fluid

m dynamic viscosity

g average volume of a microorganisms

ò porosity

l power-law variation index

y stream function

Subscripts

w conditions at the surface

f fluid

¥ conditions in the free stream

References

[1] Cheng C-Y, Natural convection heat and mass transfer of non-Newtonian power law fluids with yield stress in porous media from a vertical plate with variable wall heat and mass fluxes, , Int Commun Heat Mass Transfer 2006;33:1156-64.

[2] Hassanien IA, Variable permeability effects on mixed convection along a vertical wedge embedded in a porous medium with variable surface heat flux. Applied Mathematics and Computation, 2003;138:41-59.

[3] Bejan A, and K. R. Khair, Heat and mass transfer by natural convection in a porous medium. International Journal of Heat and Mass Transfer, 1985;28:909-18.

[4] Lee S, S. Choi US, Li S, and Eastman JA, Measuring thermal conductivity of fluids containing oxide nanoparticles. J Heat Transfer, 1999;121:280-9.

[5] Cheng P and Minkowycz WJ, Free convection about a vertical flat plate embedded in a porous medium with

application to heat transfer from a dike. Journal of Geophysical Research, 1977;82:2040-4.

[6] Kaviany M and Mittal M, An experimental study of vertical plate natural convection in porous media. Heat Transfer in Porous Media and Particulate Flows, 1985;46:175-9.

[7] Noghrehabadi A, Behseresht A, Ghalambaz M, Natural convection of nanofluid over vertical plate embedded in porous medium: prescribed surface heat flux, Appl. Math Mech - Engl Ed, 2013;34:669-86.

[8] Mahdy A, Ahmed SE, Laminar free convection over a vertical wavy surface embedded in a porous medium saturated with a nanofluid, Transp Porous Med 2012;91:423-35.

[9] Noghrehabadi A, Behseresht A and Ghalambaz M, Natural convection flow of nanofluids over a vertical cone embedded in a non-Darcy porous medium. J. Thermophysics Heat Transfer, 2013;27:334-41

[10] Nield DA, Kuznetsov AV, The Cheng-Minkowycz problem for natural convective boundary-layer flow in a porous medium saturated by a nanofluid, Int J Heat Mass Transf. 52 (2009) 5792-5.

[11] Cheng C-Y, Natural convection boundary layer flow over a truncated cone in a porous medium saturated by a nanofluid, Int Commun Heat Mass Transfer 2012;39:231-5.

[12] Abu-Nada E, Application of nanofluids for heat transfer enhancement of separated flows encountered in a backward facing step, Int J Heat Fluid Flow 2008;29:242-9.

[13] Kakać S, Pramuanjaroenkij A, Review of convective heat transfer enhancement with nanofluids, Int. J. Heat Mass Transf. 2009;52:3187-96.

[14] Das SK, S. Choi US, Yu W, Pradeep T, Nanofluids - science and technology. Hoboken: John Wiley & Sons Publishers (2007).

[15] Khan WA, Pop I, Free convection boundary layer flow past a horizontal flat plate embedded in a porous medium filled with a nanofluid, ASME J Heat Transfer 2011;133: 094501-1.

[16] Khanafer K, Vafai K, Lightstone M, Buoyancy-driven heat transfer enhancement in a two-dimensional enclosure utilizing nanofluids, Int J Heat Mass Transfer 2003;46:3639-63.

[17] Buongiorno J, Convective transport in nanofluids. J Heat Transfer 2006;128: 240-50.

[18] Khan WA, Uddin MJ, Ismail AI, Free convection of non-Newtonian nano-fluids in porous media with gyrotactic microorganisms, Transp Porous Med 2013;97:241-52.

[19] Childress S, Levandowsky M, Spiegel EA, Pattern formation in a suspension of swimming microorganisms - equations and stability theory, J. Fluid Mech. 1975;69:591-613.

[20] Geng P, Kuznetsov AV, Effect of small solid particles on the development of bioconvection plumes, Int Commun Heat Mass Transfer 2004; 31: 629-38.

[21] Hillesdon AJ, Pedley TJ, Bioconvection in suspensions of oxytactic bacteria: linear theory, J. Fluid Mech. 1996;324:223-59

[22] Becker SM, Kuznetsov AV, Avramenko AA, Numerical modeling of a falling bioconvection plume in a porous medium, Fluid Dyn Res 2004; 33:323-39

[23] Hill NA, Pedley TJ, Kessler JO, Growth of bioconvection patterns in a suspension of gyrotactic micro-organisms in a layer of finite depth, J Fluid Mech. 1989; 208: 509-43.

[24] Kuznetsov AV, Nanofluid bioconvection in water-based suspensions containing nanoparticles and oxytactic microorganisms: oscillatory instability, Nanoscale Res. Lett. 2011;6(100):1-13.

[25] Kuznetsov AV, The onset of thermo-bioconvection in a shallow fluid saturated porous layer heated from below in a suspension of oxytactic microorganisms, Eur J Mech – B/Fluids 2006;25:223-33.

[26] Geng P, Kuznetsov AV, Introducing the concept of effective diffusivity to evaluate the effect of bioconvection on small solid particles, Int J Transp. Phenom. 2005;7:321-38.

[27] Khan WA, Makinde OD, Khan ZH, MHD boundary layer flow of a nanofluid containing gyrotactic microorganisms past a vertical plate with Navier slip, Int J Heat Mass

Transfer 2014;74:285-91.

[28] Kuznetsov AV, Bio-thermal convection induced by two different species of microorganisms, Int Commun Heat Mass Transfer 2011;38:548-53.

[29] Aziz A, Khan WA, Pop I, Free convection boundary layer flow past a horizontal flat plate embedded in porous medium filled by nanofluid containing gyrotactic microorganisms, Int J Thermal Sci. 2012;56:48-57.

[30] Mutuku WN, Makinde OD, Hydromagnetic bioconvection of nanofluid over a permeable vertical plate due to gyrotactic micro- organisms, Computers & Fluids 2014; 95:88-97.

[31] Avramenko AA, Kuznetsov AV, Stability of a suspension of gyrotactic microorganisms in superimposed fluid and porous layers, Int Commun Heat Mass Transfer 2004;31:1057-66.

[32] Hady FM, Maohamed RA, Mahdy A, Omima A. Abo Zaid, Non-Darcy natural convection boundary layer flow over a vertical cone in porous media saturated with a nanofluid containing gyrotactic microorganisms with a convective boundary condition, J Nanofluids 2016;5:765-73.

[33] Ahmed SE, Mahdy A, Laminar MHD natural convection of nanofluid containing gyrotactic microorganisms over vertical wavy surface saturated non-Darcian porous media, Applied Mathematics and Mechanics 2016; 37:471-84.

[34] Mahdy A, Laminar natural convection along a vertical wavy Surface in porous media saturated by nanofluids containing gyrotactic microorganisms, J Nanofluid 2017;6(2):354-36.

[35] Hady FM, Mahdy A, Mohamed RA Omima A Abo Zaidو Effects of viscous dissipation on unsteady MHD thermo bioconvection boundary layer Flow of a nanofluid containing gyrotactic microorganisms along a stretching sheet, World J Mechanics 2016;6:505-26.

[36] Rubin SG, Graves RA, Viscous flow solution with a cubic spline approximation, Computers and Fluids 1975;3:1-36.

[37] Wang P, Kahawita R, Numerical integration of a partial differential equations using cubic spline, Int. J. Computer Mathematics 1983;13:271-86.

[38] Hsieh JC, Chen TS, Armaly BF, Nonsimilarity solutions for mixed convection from vertical surfaces in porous media, Int J Heat Mass Transfer 1993;36:1485-9.